

# Automatic differentiation for Fourier series and the radii polynomial approach

Jean-Philippe Lessard\*

J. D. Mireles James<sup>†</sup>

Julian Ransford<sup>‡</sup>

## Abstract

In this work we implement a rigorous computer-assisted technique for proving existence of periodic solutions of nonlinear differential equations with non-polynomial nonlinearities. We exploit ideas from the theory of automatic differentiation in order to formulate an augmented nonlinear system which has only polynomial nonlinearities. We validate the computation of periodic orbits for the augmented system using a combination of Fourier series analysis and the radii polynomial approach. The computer-assisted proof is obtained in a Banach space of analytic functions characterized by geometric decay of Fourier coefficients. As an application of these ideas we present the details and a number of computer-assisted results for the classical Lyapunov family of orbits in the Planar Circular Restricted Three-Body Problem (PCRTBP).

**Key words.** Rigorous numerics, automatic differentiation, Fourier series, Contraction Mapping Theorem, periodic solutions

## 1 Introduction

A fundamental issue in the qualitative theory of nonlinear differential equations is the existence question for periodic motions. The question has a global flavor and, for a given system which is not undergoing a bifurcation, can be difficult to resolve using pen and paper arguments. On the other hand numerical simulations sometimes suggest that the orbits are in fact present. In this case one looks for tools to help close the gap between numerical experiment and mathematical proof.

The present work treats a computer-assisted argument for proving the existence of periodic solutions of differential equations. The equations under consideration have non-polynomial nonlinearities. The method consists of studying a certain fixed point problem on a Banach space of Fourier coefficients, and enables us to obtain quantitative information about analytic properties of the solution such as bounds on decay rates of the Fourier coefficients, lower bounds on the size of the domain of analyticity, and bounds on derivatives of the solution. In order to implement the computer-assisted arguments for non-polynomial problems we borrow an idea from the theory of automatic differentiation which facilitates efficient composition of an unknown Fourier series with a non-polynomial vector field. This composition takes place in Fourier space, and the resulting “automatic differentiation for Fourier series” transforms the given problem into a polynomial problem in a larger number of variables. The new problem is amiable to existing methods of computer-assisted analysis. For example, we use the techniques discussed in [1] to complete the argument.

In Section 2.6 we consider a classical problem of celestial mechanics and prove the existence of a number of periodic orbits by computer-assisted methods. However before concluding the present introductory discussion, we state Theorem 1, which provides clearer insight into the nature of our results.

---

\*Université Laval, Département de Mathématiques et de Statistique, 1045 avenue de la Médecine, Québec, QC, G1V0A6, Canada. [jean-philippe.lessard@mat.ulaval.ca](mailto:jean-philippe.lessard@mat.ulaval.ca). This author was partially supported by an NSERC Discovery Grant.

<sup>†</sup>Florida Atlantic University, Department of Mathematical Sciences, Science Building, Room 234, 777 Glades Road, Boca Raton, Florida, 33431, USA. [jmirelesjames@fau.edu](mailto:jmirelesjames@fau.edu). This author was partially supported by the NSF Grant DSM - 1318172

<sup>‡</sup>Université Laval, Département de Mathématiques et de Statistique, 1045 avenue de la Médecine, Québec, QC, G1V0A6, Canada. [julian.ransford.1@ulaval.ca](mailto:julian.ransford.1@ulaval.ca). This author was partially supported by the NSERC program Undergraduate Student Research Awards (USRA).

**Theorem 1.** Let  $x(t), y(t)$  be the trigonometric polynomials

$$x(t) = a_0 + 2 \sum_{k=1}^{30} a_k \cos(k\omega t),$$

$$y(t) = -2 \sum_{k=1}^{30} b_k \sin(k\omega t),$$

with  $a_k, b_k$  the numbers given in Table 1, and  $\omega = 1.0102$ . Let  $\gamma(t) = [x(t), y(t)]$  and  $T^* = 2\pi/\omega$ . Then there is a real analytic function  $\gamma^*: [0, T^*] \rightarrow \mathbb{R}^2$  such that

1.  $\gamma^*$  is a  $T^*$ -periodic solution of the Planar Circular Restricted Three-Body Problem (PCRTBP) given in (2.1) with mass parameter  $\mu = 0.0123$ . (The PCRTBP is discussed in Section 2).
2.  $\gamma^*$  is a symmetric solution in the sense that  $\gamma_1^*(t)$  is given by a cosine series and  $\gamma_2^*(t)$  is given by a sine series.
3.  $\gamma^*$  is  $C^0$  close to  $\gamma$ . More precisely

$$\sup_{t \in [0, T^*]} |\gamma_1^*(t) - x(t)| \leq r,$$

and

$$\sup_{t \in [0, T^*]} |\gamma_2^*(t) - y(t)| \leq r,$$

with  $r = 2.5 \times 10^{-10}$ .

4. The function  $\gamma^*$  can be extended to a  $T$ -periodic analytic function on a complex strip having width at least  $\ln(1.14)/\omega \approx 0.1297$ .
5. The decay rates of the Fourier coefficients of  $\gamma^*$  satisfy the bounds

$$|a_k| \leq \frac{6.1 \times 10^{-8}}{1.14^k} \quad \text{and} \quad |b_k| \leq \frac{6.1 \times 10^{-8}}{1.14^k},$$

for  $k \geq 31$ .

The orbit itself is illustrated in Figure 6.

A few additional comments will place Theorem 1 in context within the existing literature. The PCRTBP is much studied using mathematically rigorous numerical methods and computer-assisted proofs. For example, the works of [2, 3, 4, 5, 6] employ computer-assisted topological fixed point arguments in Poincaré sections in order to prove the existence of periodic orbits. Validated numerical integration algorithms are used in order to enclose orbit segments (solutions of the initial value problem) and to solve the variational equation (compute derivatives of the flow map). The validated numerical integration algorithms facilitate mathematically rigorous evaluation of both the Poincaré map and its derivatives. If the vector field under study is  $C^k$  (in particular analytic) then one also obtains that the orbit is  $C^k$  (analytic).

Many of the numerical tools used by the authors of [4, 5, 6] are collected into the CAPD software package, a general  $C^{++}$  library for validated numerics in dynamical systems theory. We also mention that the references above include mathematically rigorous studies of heteroclinic and homoclinic connecting orbits between periodic orbits and bounds on the topological entropy of the system.

Exploiting topological arguments in a Poincaré section results in a description of the periodic orbit in terms of approximate initial conditions and approximate period. In other words, these arguments result in information given explicitly in the phase space. In contrast, Theorem 1 approximately describes the periodic solution  $\gamma^*$  in terms of trigonometric polynomials, bounds the  $C^0$  difference between the true and approximate solutions, and provides analytic bounds on the decay rate of the tail of the Fourier series representation. So the theorem provides information given explicitly in some function space. The topological and analytic methods of computer-assisted analysis complement one another, and together provide means to answer many mathematical questions concerning solutions of nonlinear differential equations.

$a_k$	$b_k$
$-9.768220550865100 \times 10^{-1}$	0
$-1.206409736493824 \times 10^{-1}$	$-2.339364883946253 \times 10^{-1}$
$-1.347990876182309 \times 10^{-2}$	$6.397869958624213 \times 10^{-3}$
$2.352585563377883 \times 10^{-3}$	$-1.790561590462826 \times 10^{-3}$
$-5.122863209781185 \times 10^{-4}$	$4.373987650320329 \times 10^{-4}$
$1.219044853784686 \times 10^{-4}$	$-1.093231659117833 \times 10^{-4}$
$-3.055685576355795 \times 10^{-5}$	$2.814155571301070 \times 10^{-5}$
$7.934843979226718 \times 10^{-6}$	$-7.428978433135244 \times 10^{-6}$
$-2.114596180594020 \times 10^{-6}$	$2.001931208169388 \times 10^{-6}$
$5.748968790488728 \times 10^{-7}$	$-5.486299609956681 \times 10^{-7}$
$-1.588047255749821 \times 10^{-7}$	$1.524601425602110 \times 10^{-7}$
$4.444105347947109 \times 10^{-8}$	$-4.286470381069696 \times 10^{-8}$
$-1.257223241334567 \times 10^{-8}$	$1.217145490467260 \times 10^{-8}$
$3.589443646509739 \times 10^{-9}$	$-3.485577927995539 \times 10^{-9}$
$-1.032912424206540 \times 10^{-9}$	$1.005555404303114 \times 10^{-9}$
$2.992744553664615 \times 10^{-10}$	$-2.919684209251029 \times 10^{-10}$
$-8.723250537889003 \times 10^{-11}$	$8.525779373911926 \times 10^{-11}$
$2.556153430692412 \times 10^{-11}$	$-2.502217287937952 \times 10^{-11}$
$-7.525630237426317 \times 10^{-12}$	$7.376943496986842 \times 10^{-12}$
$2.225016823097366 \times 10^{-12}$	$-2.183690063445679 \times 10^{-12}$
$-6.603543558111446 \times 10^{-13}$	$6.487830301502292 \times 10^{-13}$
$1.966611110890260 \times 10^{-13}$	$-1.933996961613629 \times 10^{-13}$
$-5.875220903859556 \times 10^{-14}$	$5.782732245351016 \times 10^{-14}$
$1.760271955315164 \times 10^{-14}$	$-1.733885618947898 \times 10^{-14}$
$-5.287711458070823 \times 10^{-15}$	$5.212201218470849 \times 10^{-15}$
$1.592235610864767 \times 10^{-15}$	$-1.570453382685602 \times 10^{-15}$
$-4.805263887320048 \times 10^{-16}$	$4.742351387773402 \times 10^{-16}$
$1.453325827403940 \times 10^{-16}$	$-1.435067210124585 \times 10^{-16}$
$-4.395919818622542 \times 10^{-17}$	$4.353016212240703 \times 10^{-17}$
$1.329260280567038 \times 10^{-17}$	$-1.320214388673783 \times 10^{-17}$

Figure 1: The Fourier coefficients of  $(x(t), y(t))$  of the inner most green periodic orbits on the left in Figure 6. The frequency of the orbit is  $\omega = 1.0102$ . There are  $m = 30$  Fourier coefficients per component. We could prove the existence of the orbit with  $\nu = 1.14$  and  $r = 6.1 \times 10^{-8}$ . We also proved the existence with  $\nu = 1.09$  and  $r = 2.5 \times 10^{-10}$ .

**Remark 1. (Computer-Assisted Proofs and the Radii Polynomial Approach)** The *radii polynomial approach* refers to a tool kit for carrying out *a posteriori* computer-assisted existence proofs for nonlinear operator equations

$$F(x) = 0 \tag{1.1}$$

defined on infinite-dimensional Banach spaces. The solution  $x$  may represent an invariant set of a dynamical system like a steady state, a periodic orbit, a connecting orbit, a stable manifold, etc. It could also be a minimizer of an action functional, an eigenpair of an eigenvalue problem or a solution to a boundary value problem. The radii polynomial approach consists of taking a finite-dimensional projection of (1.1), computing an approximate solution  $\bar{x}$  (e.g. using Newton’s method), constructing an approximate inverse  $A$  of  $DF(\bar{x})$ , and then proving the existence of a fixed point for the Newton-like operator

$$T(x) \stackrel{\text{def}}{=} x - AF(x) \tag{1.2}$$

by applying the Contraction Mapping Theorem (CMT) on closed balls about  $\bar{x}$ . The hypotheses of the CMT are rigorously verified by deriving a system of polynomial equations (the radii polynomials) whose coefficients carry the relevant information about the nonlinear mapping (1.2), the topology of the solution space, the given numerical approximate solution  $\bar{x}$ , and the choice of approximate inverse  $A$  for the derivative of the mapping  $F$ . The question “Is  $T$  a contraction on some neighborhood of  $\bar{x}$ ?” is reduced to a question about the zeros of the radii polynomials, and the zeros of the radii polynomials are studied via validated numerical root-finding algorithms.

The radii-polynomial approach has been applied to a host of problems in differential equations/dynamical systems theory including the study of initial value problems [7], equilibrium solutions of partial differential equations [8, 9, 10, 11, 12, 13], periodic solutions of ordinary, delay and partial differential equations [1, 14, 15, 16, 17, 18, 19], stable/unstable invariant manifolds for differential equations [20], solutions of boundary value problems such as eigenvalue/eigenfunction problems [21, 22, 23] connecting orbit problems for differential equations [24, 25], and standing wave patterns [26]. With the help of the Uniform Contraction Theorem, methods based on the radii polynomials are especially well suited for mathematically rigorous continuation schemes [27, 28, 29].

One possible criticism of this collection of methods is that it appears, at first glance, limited to problems with polynomial nonlinearities. Indeed, up to now, this approach has been applied only to problems with quadratic and cubic nonlinearities. The present work puts to rest this criticism and illustrates the wider applicability of these methods.

**Remark 2. (Automatic Differentiation, Spectral Methods, and Computer-Assisted Proof)** The question of how to efficiently compute the composition of a polynomial or power series with an elementary function appears in many numerical analysis applications. Indeed, research into algorithms for efficient multiplication of polynomials remains an active area. A classical discussion of semi-numerical algorithms for computing polynomial expansions of  $e^P$ ,  $\sin(P)$ ,  $P^k$ , etc, when  $P$  is a polynomial appears in the book of Knuth [30]. The ideas of Knuth are used in order to compute the polynomial expansion of  $f(P)$  when  $P$  is a polynomial and  $f$  is any of the “elementary functions of mathematical physics” (trigonometric functions, Bessel functions, elliptic functions, etc). This is because all such  $f$ ’s arise as solutions of low order linear differential equations. Power matching schemes applied to these differential equations reduce the cost of computing  $f(P)$  to the cost of multiplying polynomials.

The ideas discussed by Knuth in [30] are now a standard part of the Automatic Differentiation (AD) literature. A survey of the AD literature is beyond the scope of the present work and we refer for example to [31, 32, 33] for more complete exposition. Presently, we only remark that the tools of AD are used extensively in computer-assisted proofs in nonlinear analysis, especially for problems involving Taylor series expansions. The discussion in Chapters 4 and 5 of the book by Tucker [34] contains many examples and additional references to the literature. We also mention that a number of software packages and libraries for computer-assisted proof in dynamical systems theory employ AD tools for Taylor series. See for example [35, 36, 37] for discussion of the COSY software package, [38, 4, 39] for discussion of the CAPD libraries, and [40] for the INTLAB library for MATLAB.

Similar semi-numerical algorithms exist for evaluating compositions in bases other than Taylor. For example, the case of Fourier series is discussed in [41] (see the fourth remark in Section 3.3 of that reference). Here, the truncated Fourier series is treated as a trigonometric polynomial in complex conjugate variables, and recursive formulas for polynomial compositions in the style of Knuth apply directly. As mentioned in [41], the truncation error introduced by stopping at a finite order can be rigorously bound via *a posteriori* analysis and the method can be applied for computer-assisted proofs employing Fourier methods. These ideas are used in [41] in order to study invariant KAM circles in the standard map.

The paper just mentioned appears in the book [42], which is based on the proceedings of an IMA conference held at the University of Cincinnati in April of 1986. Chapter 13 of the same book contains a discussion of software tools for analysis in function spaces. Such software packages must be able to compute compositions with elementary functions as discussed above. Development of such software continues through the present and again a thorough survey of this literature is beyond the scope of the present work. More complete discussions of modern software libraries for computer-assisted proofs in Banach spaces can be found for example in [43, 44]. The packages discussed by these authors implement ideas of AD in a number of different spectral bases and include methods for rigorous bounding of roundoff and truncation errors.

In the present study we apply the ideas of AD in a slightly different way. Before we begin any numerical work, we introduce new coordinates by appending the differential equations for the composition term to the given system of differential equations. This results in an expanded system of polynomial differential equations to which we apply directly the methods of [1]. Then, our approach is similar to that of [32], but adapted for computer-assisted proofs involving Fourier series.

The remainder of the paper is organized as follows: In Sections 1.1 and 1.2, we review the basic notions of Automatic Differentiation for Taylor series and describe the situation for Fourier series. In Section 1.3, we review a spectral method for computing the Fourier coefficients of a periodic orbit and illustrate the Automatic Differentiation scheme for the familiar example of the mathematical pendulum.

In Section 2, we begin discussing the Planar Circular Restricted Three-Body Problem, the main example of the paper. We review the equations of motions and in Section 2.1, we illustrate the Automatic Differentiation scheme for the problem. Then, in Sections 2.2 and 2.3 we develop the appropriate Banach Spaces and the associated  $F(x) = 0$  problem. In Section 2.4 and 2.5, we develop the Newton-like operator and the radii polynomials for the problem. Finally in Section 2.6 we present the results of a number of computer-assisted proofs.

## 1.1 Example of Automatic Differentiation for Taylor Series

We recall the basic notion of automatic differentiation for Taylor series. Consider the formal power series

$$f(z) = \sum_{n=0}^{\infty} a_n(z - z_0)^n, \quad \text{and} \quad g(z) = \sum_{n=0}^{\infty} b_n(z - z_0)^n.$$

We denote the  $n$ -th power series coefficient by  $(f)_n = a_n$ . With  $\alpha \in \mathbb{C}$ , the standard arithmetic operations extend to power series “term by term” as

$$(f + g)_n = a_n + b_n \tag{1.3}$$

$$(\alpha f)_n = \alpha a_n \tag{1.4}$$

$$(f')_n = (n + 1)a_{n+1} \tag{1.5}$$

$$(f \cdot g)_n = \sum_{k=0}^n a_{n-k}b_k, \tag{1.6}$$

and we have that

$$f = g \quad \text{if and only if} \quad a_n = b_n \quad \text{for all } n \geq 0. \tag{1.7}$$

We now wish to extend these basic notions to include the elementary functions. For example, let  $e^z$  denote the exponential function and consider the problem of computing  $(e^f)_n$ . A natural idea would be to expand  $e^z$  using its Taylor series, so that the composition with  $f$  is computed by repeated application of Equation (1.6) in order to obtain the coefficient of  $f^k$ .

This turns out to be an inefficient way of obtaining the composition, and if we exploit further properties of the exponential function, we arrive to a more effective scheme. Note that  $(e^f)_0 = e^{f(z_0)} = e^{a_0}$ . Introducing the new power series variable

$$e^{f(z)} \stackrel{\text{def}}{=} g(z) = \sum_{n=0}^{\infty} b_n(z - z_0)^n,$$

observe that

$$\frac{d}{dz}g(z) = e^{f(z)}f'(z) = g(z)f'(z), \tag{1.8}$$

that is

$$\sum_{n=0}^{\infty} (n + 1)b_{n+1}(z - z_0)^n = \sum_{n=0}^{\infty} \left( \sum_{k=0}^n b_{n-k}(k + 1)a_{k+1} \right) (z - z_0)^n.$$

Matching like powers of  $(z - z_0)$  yields

$$(e^f)_n = \begin{cases} e^{a_0} & \text{if } n = 0 \\ \frac{1}{n} \sum_{k=1}^n k a_k (e^f)_{n-k} & \text{if } n \geq 1. \end{cases}$$

Note that we obtain the coefficients of  $e^f$  at the cost (in arithmetic operations) of multiplying two power series. The example of  $(f^\alpha)_n$  is worked out in detail in [30] using similar arguments. One can work out the power series coefficients of the composition with any elementary function. For more examples see [32], especially the discussion of Proposition 2.1 in that work.

## 1.2 An Automatic Differentiation Scheme for Fourier Series

Now suppose that  $f(z), g(z)$  are given by the Fourier series

$$f(z) = \sum_{n \in \mathbb{Z}} a_n e^{inz}, \quad \text{and} \quad g(z) = \sum_{n \in \mathbb{Z}} b_n e^{inz}.$$

Then, formally speaking, we have the term-by-term relations

$$(f + g)_n = a_n + b_n \tag{1.9}$$

$$(\alpha f)_n = \alpha a_n \tag{1.10}$$

$$(f')_n = i n a_n \tag{1.11}$$

$$(f \cdot g)_n = \sum_{k \in \mathbb{Z}} a_{n-k} b_k \tag{1.12}$$

and that

$$f = g \quad \text{if and only if} \quad a_n = b_n \quad \text{for all } n \in \mathbb{Z}. \tag{1.13}$$

In analogy with the case of power series suppose that we desire

$$g(z) \stackrel{\text{def}}{=} e^{f(z)} = \sum_{n \in \mathbb{Z}} b_n e^{inz}.$$

Returning to Equation (1.8) and in this case applying Equations (1.11), (1.12) and (1.13) we see that the desired Fourier coefficients are related by the equations

$$i n b_n = \sum_{k \in \mathbb{Z}} i k b_{n-k} a_k, \quad n \in \mathbb{Z}, \tag{1.14}$$

subject to the initial condition

$$g(0) = e^{f(0)},$$

that is

$$\sum_{n \in \mathbb{Z}} b_n = e^{\sum_{n \in \mathbb{Z}} a_n}. \tag{1.15}$$

We treat Equations (1.14), (1.15) as a system of infinitely many coupled nonlinear equations in infinitely many unknowns  $b_n$ . Truncating the system to finite order  $N$ , we can apply a Newton scheme in order to numerically approximate the desired Fourier coefficients  $b_n$  for  $-N \leq n \leq N$ . This discussion extends to other elementary functions by appending appropriate differential equations. Other spectral methods (for example Chebyshev series) can be treated by the same method.

## 1.3 Review of the Spectral Method for Periodic Orbits (with AD for Fourier Series): Example of the Mathematical Pendulum

In this section we illustrate the change of coordinates which transforms a transcendental vector field into a polynomial vector field on a higher dimensional space. We apply this change of variables in conjunction with a numerical Newton method in order to approximate the Fourier coefficients of periodic solutions of a classical transcendental nonlinear differential equation arising from mathematical physics, namely the nonlinear pendulum. The pendulum is a popular nonlinear model and appears in many introductory treatments of mechanical systems. The reader interested in a more complete discussion could consult for example the book of Fasano and Marmi [46]. The goal of the present section is to illustrate the automatic differentiation for Fourier series in a familiar example before discussing the complications associated with computer-assisted proofs.

The laws of motion for the mathematical pendulum say that the angle  $y(t)$  between the pendulum and the vertical is given by

$$y'' + \frac{g}{\ell} \sin(y) = 0. \tag{1.16}$$

We choose units for the problem so that  $g/\ell = 1$  and compute the Fourier series representation for periodic solutions for the problem. Introducing the coordinates  $u_1 = y$  and  $u_2 = y'$  gives the first order system

$$\begin{aligned} u_1' &= u_2 \\ u_2' &= -\sin(u_1). \end{aligned}$$

We exploit the symmetry of the problem and look for solutions of the form

$$u_1(t) = a_0 + 2 \sum_{n=1}^{\infty} a_n \cos(n\omega t), \quad \text{and} \quad u_2(t) = 2 \sum_{n=1}^{\infty} b_n \sin(n\omega t),$$

where  $\omega$  is the frequency of the periodic solution.

### 1.3.1 Equivalent $F(x) = 0$ for the Pendulum

In order to formulate the problem as an  $F(x) = 0$  problem on a sequence spaces of Fourier coefficients, we must project the sine function onto a Fourier basis. Here we illustrate the automatic differentiation scheme. We begin by introducing the variables

$$u_3 = \sin(u_1), \quad \text{and} \quad u_4 = \cos(u_1).$$

Differentiating with respect to time gives  $u_3' = \cos(u_1)u_1' = u_4u_2$ , and  $u_4' = -\sin(u_1)u_1' = -u_3u_2$ . Then finding a periodic solution of the mathematical pendulum is equivalent to finding a solution of

$$\left. \begin{aligned} u_1' &= u_2 \\ u_2' &= -u_3 \\ u_3' &= u_2u_4 \\ u_4' &= -u_2u_3 \end{aligned} \right\} \quad (1.17)$$

subject to the scalar constraints (initial conditions)

$$u_3(0) = \sin(u_1(0)), \quad \text{and} \quad u_4(0) = \cos(u_1(0)).$$

These constraints ensure that  $u_3$  and  $u_4$  are the sine and cosine of  $u_1$ , and not just some linear combination of the sine and cosine.

Let

$$u_3(t) = c_0 + 2 \sum_{n=1}^{\infty} c_n \cos(n\omega t), \quad \text{and} \quad u_4(t) = d_0 + 2 \sum_{n=1}^{\infty} d_n \cos(n\omega t).$$

Plugging the Fourier expansions into Equation (1.17) leads to

$$-2 \sum_{n=1}^{\infty} n\omega a_n \sin(n\omega t) = 2 \sum_{n=1}^{\infty} b_n \sin(n\omega t) \quad (1.18)$$

$$2 \sum_{n=1}^{\infty} n\omega b_n \cos(n\omega t) = -c_0 - 2 \sum_{n=1}^{\infty} c_n \cos(n\omega t) \quad (1.19)$$

$$-2 \sum_{n=1}^{\infty} n\omega c_n \sin(n\omega t) = 2 \sum_{n=1}^{\infty} (b * d)_n \sin(n\omega t) \quad (1.20)$$

$$-2 \sum_{n=1}^{\infty} n\omega d_n \sin(n\omega t) = -2 \sum_{n=1}^{\infty} (b * c)_n \sin(n\omega t), \quad (1.21)$$

where the notation  $a * b$  denotes the discrete convolution between  $a$  and  $b$  given component-wise by the right-hand side of (1.12). To evaluate the discrete convolutions, we introduce negative indices as

$$b_{-n} \stackrel{\text{def}}{=} -b_n, \quad c_{-n} \stackrel{\text{def}}{=} c_n \quad \text{and} \quad d_{-n} \stackrel{\text{def}}{=} d_n.$$

We solve (1.18), (1.19), (1.20) and (1.21) subject to the constraints

$$c_0 + 2 \sum_{n=1}^{\infty} c_n = \sin \left( a_0 + 2 \sum_{n=1}^{\infty} a_n \right), \quad \text{and} \quad d_0 + 2 \sum_{n=1}^{\infty} d_n = \cos \left( a_0 + 2 \sum_{n=1}^{\infty} a_n \right). \quad (1.22)$$

**Remark 3.** Note that Equation (1.19) imposes that  $c_0 = 0$ . Moreover  $b_0 = 0$  because  $u_2(t)$  is a sine series. On the other hand  $a_0$  and  $d_0$  are unconstrained variables. Then two scalar conditions are needed in order to determine a unique solution, and these are provided by (1.22). Then the system leads to an appropriate number of equations and unknowns. Also note that we are not imposing the known fact that for the pendulum  $a_0 = \pi n$  for some  $n \in \mathbb{Z}$ . Instead, we will solve for the average as this will typically be necessary in other application problems. Indeed, there are other symmetries of the problem that we are ignoring.

Let

$$a \stackrel{\text{def}}{=} \{a_n\}_{n=0}^{\infty}, \quad b \stackrel{\text{def}}{=} \{b_n\}_{n=1}^{\infty}, \quad c \stackrel{\text{def}}{=} \{c_n\}_{n=1}^{\infty}, \quad d \stackrel{\text{def}}{=} \{d_n\}_{n=0}^{\infty} \quad \text{and} \quad x \stackrel{\text{def}}{=} (a, b, c, d),$$

and consider the system of coupled equations

$$\begin{aligned} \eta_1(x) &\stackrel{\text{def}}{=} 2 \sum_{n=1}^{\infty} c_n - \sin \left( a_0 + 2 \sum_{n=1}^{\infty} a_n \right) = 0, \\ \eta_2(x) &\stackrel{\text{def}}{=} d_0 + 2 \sum_{n=1}^{\infty} d_n - \cos \left( a_0 + 2 \sum_{n=1}^{\infty} a_n \right) = 0, \end{aligned}$$

and

$$\begin{aligned} f_1(x) &\stackrel{\text{def}}{=} \{n\omega a_n + b_n\}_{n \geq 1} = 0, \\ f_2(x) &\stackrel{\text{def}}{=} \{n\omega b_n + c_n\}_{n \geq 1} = 0, \\ f_3(x) &\stackrel{\text{def}}{=} \{n\omega c_n + (b * d)_n\}_{n \geq 1} = 0, \\ f_4(x) &\stackrel{\text{def}}{=} \{n\omega d_n - (b * c)_n\}_{n \geq 1} = 0. \end{aligned}$$

Hence, looking for periodic solutions of the mathematical pendulum (1.16) is equivalent to finding solutions  $x$  of the infinite-dimensional system of algebraic equations

$$F(x) \stackrel{\text{def}}{=} \begin{pmatrix} \eta_1(x) \\ \eta_2(x) \\ f_1(x) \\ f_2(x) \\ f_3(x) \\ f_4(x) \end{pmatrix} = 0, \quad (1.23)$$

where  $x$  is an element of an infinite-dimensional space  $X$ , which we do not specify in the present section.

Truncating the system (1.23) to  $m$  modes provides a system of  $4m + 2$  equations in as many unknowns  $a_0, d_0, a_1, \dots, a_m, b_1, \dots, b_m, c_1, \dots, c_m$ , and  $d_1, \dots, d_m$ . The truncated system can be solved by a numerical Newton method. The reader interested in the numerical implementation can see the MATLAB program [47]. A cylinder of periodic orbits for the pendulum is illustrated in Figure 2.

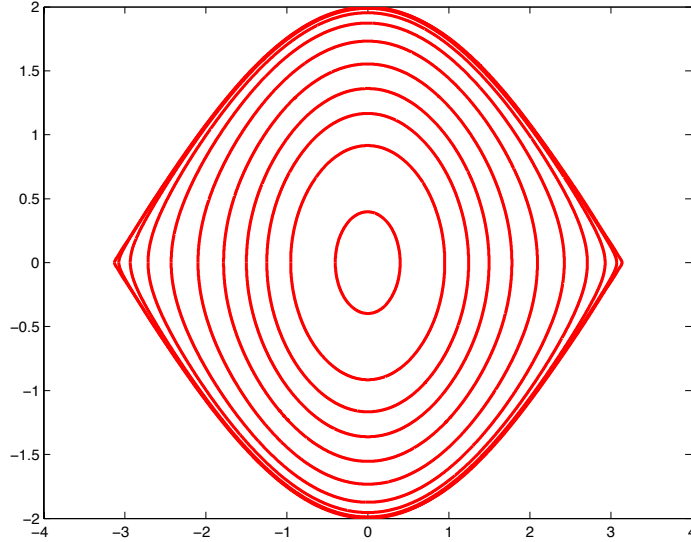


Figure 2: The figure illustrates  $u_1$  versus  $u_2$  for a “cylinder” of periodic orbits with frequencies chosen  $0.15392 \leq \omega \leq 0.99$ , that is, for periods starting near  $2\pi$  and growing as large as 40.8224. The plot shows the familiar shape of the pendulum phase space with long periodic orbits limiting to the heteroclinic separatrix.

**Remark 4.** Note that the frequency  $\omega$  is also an unknown in the problem. In a dissipative system (where periodic orbits are typically isolated) we would solve for  $\omega$  as a problem variable. This would require the addition of one more scalar equation, or phase condition. For example, one can append a Poincaré phase condition (e.g. see [1] for a fuller discussion of phase conditions in the Fourier space setting). On the other hand, periodic orbits of Hamiltonian systems are typically found in one parameter families parametrized by energy (This classical result is a simple consequence of the Implicit Function Theorem. For the details, see for example Chapter 5.E of [45]). The family of periodic orbits forms an invariant cylinder and the typical situation is that the cylinder satisfies a twist condition, that is its frequency is a monotonic function of energy. Then, instead of fixing the energy and solving for the corresponding periodic orbit, we are free to fix the frequency and look for the corresponding periodic orbit in the energy cylinder. In the context of the current set up, this simplifies the problem by simply removing one variable from the problem. On the other hand, if one wishes to prove the existence of a periodic orbit in a specific energy level, then the energy function may be added as a scalar constraint and the frequency left as a problem variable.

### 1.3.2 Numerical Results and Comparisons

It is well known that the exact solution of the initial value problem for the pendulum equation with  $y(0) = y_0$  and  $y'(0) = 0$  is given by

$$y(t) = 2 \arcsin \left( \sqrt{m} \operatorname{ellipj}(K(m) - t, m) \right) \quad (1.24)$$

where  $\operatorname{ellipj}(x, n)$  is the Jacobi elliptic function, where

$$m \stackrel{\text{def}}{=} \sin^2 \left( \frac{y_0}{2} \right),$$

and where

$$K(m) \stackrel{\text{def}}{=} \int_0^1 \frac{dz}{\sqrt{(1-z^2)(1-mz^2)}}$$

is the elliptic integral of the first kind. (Again we refer Section 3.3 of the book by Fasano and Marmi [46]). The Jacobi elliptic function and the elliptic integral have standard function calls in MATLAB and we can compare the solution by our automatic differentiation scheme to the exact solution given by Equation (1.24). Some results are reported in Table 1. The reader interested in the numerical implementation can find the source codes at [47].

$\omega$	$T$	Error $N = 20$	Error $N = 30$	Error $N = 40$	Error $N = 50$	Error $N = 60$
0.9387	6.6935	$1.11 \times 10^{-14}$	$5.468 \times 10^{-15}$	NA	NA	NA
0.889	7.0701	$4.59 \times 10^{-14}$	$5.77 \times 10^{-15}$	NA	NA	NA
0.828	7.589	$8.67 \times 10^{-12}$	$6.44 \times 10^{-15}$	NA	NA	NA
0.828	7.589	$8.67 \times 10^{-12}$	$6.44 \times 10^{-15}$	NA	NA	NA
0.739	8.511	$2.17 \times 10^{-9}$	$3.96 \times 10^{-14}$	NA	NA	NA
0.621	10.13	$4.49 \times 10^{-7}$	$2.96 \times 10^{-11}$	$5.99 \times 10^{-14}$	$1.25 \times 10^{-14}$	NA
0.494	12.72	$5.13 \times 10^{-5}$	$3.1 \times 10^{-8}$	$1.7 \times 10^{-11}$	$1.5 \times 10^{-13}$	$2.2 \times 10^{-14}$
0.368	17.07	0.005	$2.34 \times 10^{-5}$	$9.6 \times 10^{-8}$	$3.67 \times 10^{-10}$	$1.06 \times 10^{-12}$

Table 1: The table reports the maximum point-wise difference between the value of the solution of Equation (1.16) computed in two different ways: first by solving the system equations in Fourier space using a Newton method and then by evaluating Equation (1.24). The difference is evaluated at 100 times  $0 \leq t \leq T = 2\pi/\omega$ . The table reports on results for 8 values of  $6.6935 \leq T \leq 17.07$  and in each case we list the error between the Fourier solution and the analytic solution for various truncation dimensions  $N$ . When an entry of the table reads NA it simply means that we do not report the results as the error was sufficiently small for a smaller number of modes. We also note that with  $N = 70$  modes, the error in the last computation is approximately  $1.6 \times 10^{-13}$ .

## 2 Planar Circular Restricted Three-Body Problem

A classical problem in celestial mechanics is the Planar Circular Restricted Three-Body Problem (PCRTBP). We provide a brief description of the problem and refer the reader to the book by Meyer and Hall [45] for a more complete treatment and discussion of the literature. In this problem, one considers two bodies of mass  $m_1 > m_2 > 0$  moving in a circular Keplerian orbit. These are called the primary and secondary bodies respectively. Let  $\mu = m_1/(m_1 + m_2)$  denote the *mass ratio* and choose coordinates so that the circular orbit lies in the  $X, Y$  plane with center of mass at the origin. Since orbits are circular, the line determined by the masses passes through the center of mass (that is the origin) and rotates at a constant frequency. One can define a rotating coordinate system with the  $x$  axis determined by the line between the two masses. The coordinates are rescaled so that distances between the massive bodies and the origin are  $\mu$  and  $1 - \mu$  respectively. Hence the bodies are positioned at  $-\mu$  and  $1 - \mu$  along the fixed rotating line  $x$ . This situation is illustrated in Figures 3 and 4.

The massive bodies are now referred to collectively as “the primaries”. A third and massless particle (sometimes called a “test particle”) is placed *in the plane of motion* of the primaries. The massless particle moves in the resulting gravitational field without disturbing the Keplerian motion of the primaries, that is without creating any gravitational field of its own. Writing Newton’s laws for the motion of the massless particle (transformed to the non-inertial co-rotating reference frame) gives the system of two second order ordinary differential equations

$$\begin{cases} x'' = 2y' + \frac{\partial V}{\partial x} \\ y'' = -2x' + \frac{\partial V}{\partial y}, \end{cases} \quad (2.1)$$

where

$$V(x, y) \stackrel{\text{def}}{=} \frac{1}{2}(x^2 + y^2) + \frac{1 - \mu}{r_1(x, y)} + \frac{\mu}{r_2(x, y)}$$

and

$$\begin{cases} r_1(x, y) \stackrel{\text{def}}{=} \sqrt{(x + \mu)^2 + y^2} \\ r_2(x, y) \stackrel{\text{def}}{=} \sqrt{(x - 1 + \mu)^2 + y^2}. \end{cases}$$

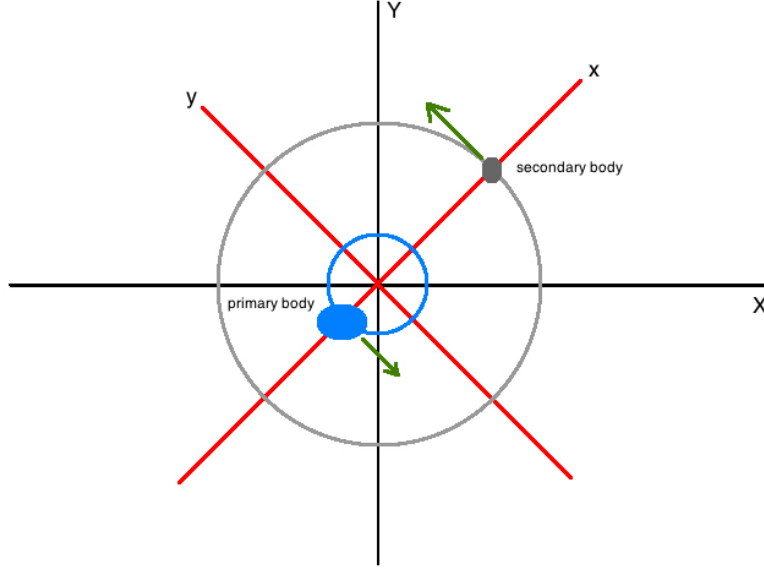


Figure 3: A massive primary body and a smaller secondary body in circular motion. The  $X, Y$  coordinates (black axes) illustrate the standard Galilean center of mass coordinate frame. The  $x, y$  coordinates (red axes) illustrate a co-rotating frame. In the rotating frame, the primary and secondary bodies lie always on the  $x$ -axis.

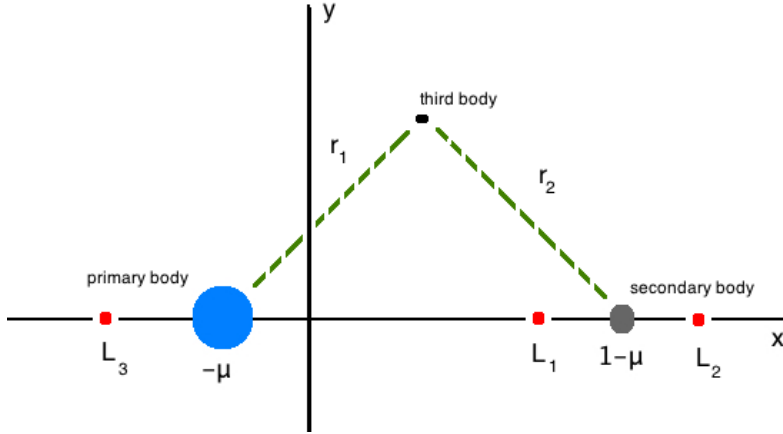


Figure 4: In the co-rotating (non-inertial) frame, we introduce a third and massless particle. The magnitude of the distance from the massless particle to the primary body is  $r_1$  and the magnitude of the distance from the massless particle to the secondary particle is  $r_2$ . The massless particle is influenced by the gravitational fields of the primary and secondary bodies, however the massless body does not affect the orbits of the massive bodies. In the rotating reference frame, there are three collinear equilibrium points on the  $x$ -axis which are denoted  $L_1, L_2, L_3$ .

Letting  $x_1 \stackrel{\text{def}}{=} x$ ,  $x_2 \stackrel{\text{def}}{=} x'$ ,  $x_3 \stackrel{\text{def}}{=} y$  and  $x_4 \stackrel{\text{def}}{=} y'$ , the system (2.1) becomes

$$\begin{cases} x'_1 = x_2 \\ x'_2 = 2x_4 + \frac{\partial V}{\partial x} \\ x'_3 = x_4 \\ x'_4 = -2x_2 + \frac{\partial V}{\partial y}. \end{cases} \quad (2.2)$$

The system has at most five equilibrium solutions, three of which lie on the  $x$ -axis. The three equilibrium points on the  $x$ -axis are called the collinear equilibria and are denoted  $L_1, L_2, L_3$ . The collinear equilibria have saddle-center stability. The center manifold of each collinear equilibrium point is foliated by a family of hyperbolic periodic orbits referred to as the Lyapunov orbits. The Lyapunov orbits are parametrized by energy/frequency. These orbits are the main point of study in the remainder of the present work.

## 2.1 Equivalent Polynomial Vector Field Formulation and the Automatic Differentiation of Fourier Series for the CRTBP

Next, we want to transform (2.2) into a polynomial system. In order to do so, we first take the partial derivatives of  $V(x, y)$ , that is

$$\begin{cases} \frac{\partial V}{\partial x} = x - \frac{(1-\mu)(x+\mu)}{((x+\mu)^2+y^2)^{\frac{3}{2}}} - \frac{\mu(x-1+\mu)}{((x-1+\mu)^2+y^2)^{\frac{3}{2}}} \\ \frac{\partial V}{\partial y} = y - \frac{(1-\mu)y}{((x+\mu)^2+y^2)^{\frac{3}{2}}} - \frac{\mu y}{((x-1+\mu)^2+y^2)^{\frac{3}{2}}}. \end{cases}$$

We then let  $x_5 \stackrel{\text{def}}{=} \frac{1}{\sqrt{(x_1+\mu)^2+x_3^2}}$  and  $x_6 \stackrel{\text{def}}{=} \frac{1}{\sqrt{(x_1-1+\mu)^2+x_3^2}}$ . By differentiating these with respect to  $t$ , we get

$$x_5'(t) = -\frac{(x+\mu)x' + yy'}{((x+\mu)^2+y^2)^{\frac{3}{2}}} = -x_5^3((x_1+\mu)x_2 + x_3x_4)$$

and

$$x_6'(t) = -\frac{(x-1+\mu)x' + yy'}{((x-1+\mu)^2+y^2)^{\frac{3}{2}}} = -x_6^3((x_1-1+\mu)x_2 + x_3x_4).$$

Plugging  $x_5$  and  $x_6$  into (2.2) and adding our expressions for  $x_5'$  and  $x_6'$  into the mix, we get our final quintic polynomial vector field

$$\begin{cases} x_1' = x_2 \\ x_2' = 2x_4 + x_1 - (1-\mu)(x_1+\mu)x_5^3 - \mu x_6^3(x_1-1+\mu) \\ x_3' = x_4 \\ x_4' = -2x_2 + x_3 - (1-\mu)x_3x_5^3 - \mu x_3x_6^3 \\ x_5' = -x_5^3((x_1+\mu)x_2 + x_3x_4) \\ x_6' = -x_6^3((x_1-1+\mu)x_2 + x_3x_4), \end{cases} \quad (2.3)$$

where the extra conditions

$$x_5(0) = \frac{1}{\sqrt{(x_1(0)+\mu)^2+x_3(0)^2}} \quad (2.4)$$

$$x_6(0) = \frac{1}{\sqrt{(x_1(0)-1+\mu)^2+x_3(0)^2}} \quad (2.5)$$

need to be imposed.

Let us now introduce the operator (1.1) whose solutions correspond to periodic solutions of (2.1). Once this operator is introduced, we use the theory of Section 3 of [1] to compute rigorously its solutions.

## 2.2 The Operator Equation $F(\mathbf{a}) = \mathbf{0}$

Since we are looking for periodic solutions, we assume that the  $x_j$ 's can be represented using Fourier series and our job is thus to find the Fourier coefficients. As we all know, series of exponentials can be broken down into sine and cosine series. Given a fixed period  $2\pi/\omega$ , where  $\omega$  is the frequency, we look for periodic orbits of (2.1) satisfying  $x'(0) = y(0) = 0$ . Because (2.2) is Hamiltonian, there are some symmetries and we have that  $x_1, x_4, x_5, x_6$  are cosine series and  $x_2, x_3$  are sine series, that is

$$x_j(t) = \sum_{k \in \mathbb{Z}} (a_j)_k e^{ik\omega t} = (a_j)_0 + 2 \sum_{k=1}^{\infty} (a_j)_k \cos(k\omega t), \quad \text{for } j = 1, 4, 5, 6$$

with  $(a_j)_{-k} \stackrel{\text{def}}{=} (a_j)_k \in \mathbb{R}$  for  $j = 1, 4, 5, 6$ , and

$$x_j(t) = \sum_{k \in \mathbb{Z}} i(a_j)_k e^{ik\omega t} = -2 \sum_{k=1}^{\infty} (a_j)_k \sin(k\omega t), \quad \text{for } j = 2, 3,$$

with  $(a_j)_{-k} \stackrel{\text{def}}{=} -(a_j)_k \in \mathbb{Z}$  for  $j = 2, 3$ . While the cosine and sine series only have positive indices, it is important to also consider negative indices, so that we can calculate discrete convolutions the usual way. For instance,

$$x_1(t)x_2(t)x_5^3(t) = \sum_{k \in \mathbb{Z}} (a_1 ia_2 a_5^3)_k e^{ik\omega t} = -2 \sum_{k=1}^{\infty} (a_1 a_2 a_5^3)_k \sin(k\omega t),$$

where

$$(a_1 a_2 a_5^3)_k = \sum_{\substack{k_1+k_2+k_3+k_4+k_5=k \\ k_i \in \mathbb{Z}}} (a_1)_{k_1} (a_2)_{k_2} (a_5)_{k_3} (a_5)_{k_4} (a_5)_{k_5},$$

and where  $(a_1 a_2 a_5^3)_{-k} = -(a_1 a_2 a_5^3)_k$  follows from the fact that  $(a_1)_{-k} = (a_1)_k$ ,  $(a_2)_{-k} = -(a_2)_k$  and  $(a_5)_{-k} = (a_5)_k$ .

Now that we have a Fourier representation of our solutions, all we need to do is find the coefficients. To do this, we first substitute our series into (2.3). Since the equations must be verified for all values of  $t$ , we have that our vector function solves (2.3) if and only if the coefficients correspond on both sides of the equation. So, by putting everything on the same side of the equation, we must solve  $(F_j)_k = 0$  for  $j = 1, \dots, 6$ , where for  $k \geq 1$ ,

$$\begin{cases} (F_1)_k \stackrel{\text{def}}{=} k\omega(a_1)_k - (a_2)_k \\ (F_2)_k \stackrel{\text{def}}{=} k\omega(a_2)_k + 2(a_4)_k + (a_1) - (1-\mu)(a_1 a_5^3)_k - (\mu - \mu^2)(a_5^3)_k \\ \quad - \mu(a_1 a_6^3)_k + (\mu - \mu^2)(a_6^3)_k \\ (F_3)_k \stackrel{\text{def}}{=} k\omega(a_3)_k + (a_4)_k \\ (F_4)_k \stackrel{\text{def}}{=} k\omega(a_4)_k + 2(a_2)_k - (a_3)_k + (1-\mu)(a_3 a_5^3)_k + \mu(a_3 a_6^3)_k \\ (F_5)_k \stackrel{\text{def}}{=} k\omega(a_5)_k + (a_1 a_2 a_5^3)_k + (a_3 a_4 a_5^3)_k + \mu(a_2 a_5^3)_k \\ (F_6)_k \stackrel{\text{def}}{=} k\omega(a_6)_k + (a_1 a_2 a_6^3)_k + (a_3 a_4 a_6^3)_k + (\mu - 1)(a_2 a_6^3)_k. \end{cases} \quad (2.6)$$

Since  $x_2, x_3 \in \mathbb{R}$  are expressed as sine series, their constant Fourier coefficients, given respectively by  $(a_2)_0$  and  $(a_3)_0$ , are zero. However, to simplify the analysis, we consider  $(a_2)_0$  and  $(a_3)_0$  as variables and impose them to be zero within the operator. Therefore, for  $k = 0$ , we set

$$\begin{cases} (F_1)_0 \stackrel{\text{def}}{=} (a_2)_0 \\ (F_2)_0 \stackrel{\text{def}}{=} 2(a_4)_0 + (a_1) - (1-\mu)(a_1 a_5^3)_0 - (\mu - \mu^2)(a_5^3)_0 \\ \quad - \mu(a_1 a_6^3)_0 + (\mu - \mu^2)(a_6^3)_0 \\ (F_3)_0 \stackrel{\text{def}}{=} (a_4)_0 \\ (F_4)_0 \stackrel{\text{def}}{=} (a_3)_0 \\ (F_5)_0 \stackrel{\text{def}}{=} \eta_1 \\ (F_6)_0 \stackrel{\text{def}}{=} \eta_2, \end{cases} \quad (2.7)$$

where  $\eta_1$  and  $\eta_2$  depends on the value of  $x_1(0) + \mu$ . More explicitly,

$$\eta_1 \stackrel{\text{def}}{=} \begin{cases} x_5(0)(x_1(0) + \mu) - 1, & \text{if } x_1(0) + \mu > 1 \\ x_5(0)(x_1(0) + \mu) - 1, & \text{if } x_1(0) + \mu \in (0, 1) \\ -x_5(0)(x_1(0) + \mu) - 1, & \text{if } x_1(0) + \mu < 0 \end{cases} \quad (2.8)$$

$$\eta_2 \stackrel{\text{def}}{=} \begin{cases} x_6(0)(x_1(0) + \mu - 1) - 1, & \text{if } x_1(0) + \mu > 1 \\ -x_6(0)(x_1(0) + \mu - 1) - 1, & \text{if } x_1(0) + \mu \in (0, 1) \\ -x_6(0)(x_1(0) + \mu - 1) - 1, & \text{if } x_1(0) + \mu < 0, \end{cases} \quad (2.9)$$

where  $x_j(0) = (a_j)_0 + 2 \sum_{k \geq 1} (a_j)_k$  for  $j = 1, 5, 6$ . In all cases,  $\eta_1 = 0$  ensures that (2.4) holds while  $\eta_2 = 0$  ensures that (2.5) holds.

For  $j = 1, \dots, 6$ , let  $a_j \stackrel{\text{def}}{=} ((a_j)_k)_{k \geq 0}$  and  $F_j \stackrel{\text{def}}{=} ((F_j)_k)_{k \geq 0}$ . Moreover, set

$$a \stackrel{\text{def}}{=} (a_1, a_2, a_3, a_4, a_5, a_6) \quad \text{and} \quad F \stackrel{\text{def}}{=} (F_1, F_2, F_3, F_4, F_5, F_6).$$

From the above discussions, computing periodic solutions of the planar circular restricted 3-body problem is equivalent to finding solutions of

$$F(a) = 0, \tag{2.10}$$

where the coefficients of  $F(a)$  are given by (2.7) and (2.6).

Let us now introduce the Banach space  $X$  on which we look for solutions of (2.10).

### 2.3 The Banach Space $X$

Since (2.3) is a real analytic vector field, any periodic solution is real analytic. Therefore, the Fourier coefficients of the components of any periodic solution decay to zero exponentially fast. This fundamental fact justifies the choice of Banach space on which we solve (2.10). Given an exponential decay rate  $\nu \geq 1$ , let

$$\ell_\nu^1 \stackrel{\text{def}}{=} \left\{ c = (c_k)_{k \geq 0} \mid c_k \in \mathbb{R} \quad \text{and} \quad \|c\|_\nu \stackrel{\text{def}}{=} \sum_{k \geq 0} |c_k| \nu^k < \infty \right\}.$$

A consequence of the definition of the above space is that a sequence  $c \in \ell_\nu^1$  must have that its coefficients decay (at infinity) to zero faster than the geometric decay rate  $\nu^{-k}$ . Define the Banach space

$$X \stackrel{\text{def}}{=} (\ell_\nu^1)^6 = \left\{ a = (a_1, a_2, a_3, a_4, a_5, a_6) \mid a_j \in \ell_\nu^1, \quad j = 1, \dots, 6 \right\} \tag{2.11}$$

endowed with the norm

$$\|a\|_X = \max_{j=1, \dots, 6} \{\|a_j\|_\nu\}.$$

To derive the bounds necessary to prove existence of solutions of (2.10) within the Banach space  $X$  defined by (2.11), we will use the following fundamental result.

**Lemma 2.** *Let  $\nu \geq 1$  and  $a_1, a_2 \in \ell_\nu^1$ . Consider any bi-infinite sequences  $\tilde{a}_1 = ((\tilde{a}_1)_k)_{k \in \mathbb{Z}}$ ,  $\tilde{a}_2 = ((\tilde{a}_2)_k)_{k \in \mathbb{Z}}$  with indices so that  $(\tilde{a}_j)_k = (a_j)_k$  and  $|(\tilde{a}_j)_{-k}| = |(a_j)_k|$  for  $j = 1, 2$  and for all  $k \geq 0$ . Then  $((\tilde{a}_1 * \tilde{a}_2)_k)_{k \geq 0} \in \ell_\nu^1$  and*

$$\|((\tilde{a}_1 * \tilde{a}_2)_k)_{k \geq 0}\|_\nu \leq 4\|a_1\|_\nu \|a_2\|_\nu. \tag{2.12}$$

*Proof.*

$$\begin{aligned} \|((\tilde{a}_1 * \tilde{a}_2)_k)_{k \geq 0}\|_\nu &= \sum_{k \geq 0} |(\tilde{a}_1 * \tilde{a}_2)_k| \nu^k = \sum_{k \geq 0} \left| \sum_{\substack{k_1 + k_2 = k \\ k_1, k_2 \in \mathbb{Z}}} (\tilde{a}_1)_{k_1} (\tilde{a}_2)_{k_2} \right| \nu^k \\ &\leq \sum_{k \geq 0} \sum_{\substack{k_1 + k_2 = k \\ k_1, k_2 \in \mathbb{Z}}} |(\tilde{a}_1)_{k_1}| |(\tilde{a}_2)_{k_2}| \nu^k \leq 4 \sum_{k \geq 0} \sum_{\substack{k_1 + k_2 = k \\ k_1, k_2 \geq 0}} |(a_1)_{k_1}| \nu^{k_1} |(a_2)_{k_2}| \nu^{k_2} \\ &\leq 4 \left( \sum_{k_1 \geq 0} |(a_1)_{k_1}| \nu^{k_1} \right) \left( \sum_{k_2 \geq 0} |(a_2)_{k_2}| \nu^{k_2} \right) = 4\|a_1\|_\nu \|a_2\|_\nu. \quad \square \end{aligned}$$

**Remark 5.** *The bound (2.12) holds for discrete convolutions involving any combination of cosine sequences (that is sequences extended over negative indices using the rule  $b_{-k} = b_k$ ) and sine sequences (extended over negative indices using the rule  $b_{-k} = -b_k$ ).*

Instead of solving (2.10) directly, we introduce a fixed point equation of the form  $T(a) = a - AF(a)$  (where  $A$  is an injective linear operator to be defined) whose fixed points are in one-to-one correspondence with the zeroes of  $F$ .

## 2.4 Definition of the Approximate Inverse Operator $A$

Assume that using a finite-dimensional projection  $F^{(m)} : \mathbb{R}^{6m} \rightarrow \mathbb{R}^{6m}$  of (2.10), we applied Newton's method to find a numerical solution  $\bar{a} = (\bar{a}_1, \dots, \bar{a}_6) \in \mathbb{R}^{6m}$  such that  $F^{(m)}(\bar{a}) \approx 0$ . Denote  $DF(\bar{a}) = \{D_{a_i} F_j(\bar{a})\}_{i,j=1}^6$ , where each component of  $DF(\bar{a})$  is a linear operator such that  $D_{a_i} F_j(\bar{a}) : \ell_\nu^1 \rightarrow \ell_\nu^1$ , are linear operators with  $\nu' < \nu$ . We first approximate  $DF(\bar{a})$  with the operator  $A^\dagger = \left\{ A_{j,a_i}^\dagger \right\}_{i,j=1}^6$  which acts on  $b = (b_i)_{i=1}^6$  component-wise as  $(A^\dagger b)_j = \sum_{i=1}^6 A_{j,a_i}^\dagger b_i$  for  $j = 1, \dots, 6$ , where  $A_{j,a_i}^\dagger b_i \in \ell_{\nu'}^1$  is defined component-wise by

$$\left( A_{j,a_i}^\dagger b_i \right)_k = \begin{cases} \left( D_{a_i} F_j^{(m)}(\bar{a}) b_i^{(m)} \right)_k, & 0 \leq k < m \\ \delta_{i,j} \omega k (b_i)_k, & k \geq m. \end{cases}$$

Let  $A^{(m)}$  be a finite-dimensional approximate inverse of  $DF^{(m)}(\bar{a})$  which is obtained numerically. Define the decomposition  $A^{(m)} = \left\{ A_{j,a_i}^{(m)} \right\}_{i,j=1}^6 \in \mathbb{R}^{6m} \times \mathbb{R}^{6m}$ , where  $A_{j,a_i}^{(m)} \in \mathbb{R}^m \times \mathbb{R}^m$ . We define the approximate inverse  $A$  of the infinite-dimensional operator  $DF(\bar{a})$  by  $A = \{A_{j,a_i}\}_{i,j=1}^6$ , that is

$$A = \begin{pmatrix} A_{1,a_1} & A_{1,a_2} & A_{1,a_3} & A_{1,a_4} & A_{1,a_5} & A_{1,a_6} \\ A_{2,a_1} & A_{2,a_2} & A_{2,a_3} & A_{2,a_4} & A_{2,a_5} & A_{2,a_6} \\ A_{3,a_1} & A_{3,a_2} & A_{3,a_3} & A_{3,a_4} & A_{3,a_5} & A_{3,a_6} \\ A_{4,a_1} & A_{4,a_2} & A_{4,a_3} & A_{4,a_4} & A_{4,a_5} & A_{4,a_6} \\ A_{5,a_1} & A_{5,a_2} & A_{5,a_3} & A_{5,a_4} & A_{5,a_5} & A_{5,a_6} \\ A_{6,a_1} & A_{6,a_2} & A_{6,a_3} & A_{6,a_4} & A_{6,a_5} & A_{6,a_6} \end{pmatrix}.$$

The linear operator  $A$  acts on  $b = (b_i)_{i=1}^6 \in X = (\ell_\nu^1)^6$  component-wise as  $(Ab)_j = \sum_{i=1}^6 A_{j,a_i} b_i \in \ell_\nu^1$  for  $j = 1, \dots, 6$  with  $A_{j,a_i} b_i \in \ell_\nu^1$  defined component-wise by

$$\left( A_{j,a_i} b_i \right)_k = \begin{cases} \left( A_{j,a_i}^{(m)} b_i^{(m)} \right)_k, & 0 \leq k < m \\ \frac{\delta_{i,j}}{\omega k} (b_i)_k, & k \geq m. \end{cases} \quad (2.13)$$

Having defined  $A$  piece by piece, we can now define the Newton-like operator by

$$T(a) = a - AF(a). \quad (2.14)$$

We show existence of fixed points of  $T$  with the radii polynomial approach.

## 2.5 The Radii Polynomial Approach for Periodic Orbits

In this section, we essentially follow the approach introduced in Section 3 of [1]. This is why we omit many technical details.

Given  $\bar{a} = (\bar{a}_1, \dots, \bar{a}_6)$ , with  $\bar{a}_j = ((\bar{a}_j)_{-m+1}, \dots, (\bar{a}_j)_{m-1})$ , define the bounds

$$Y = (Y_1, \dots, Y_6) \in \mathbb{R}^6 \\ Z(r) = (Z_1(r), \dots, Z_6(r)) \in \mathbb{R}^6$$

such that

$$\left\| (T(\bar{a}) - \bar{a})_j \right\|_\nu \leq Y_j, \quad \sup_{b,c \in B(r)} \left\| (DT_j(\bar{a} + b)c) \right\|_\nu \leq Z_j(r), \quad \text{for } j = 1, \dots, 6. \quad (2.15)$$

The following result is proved in [1].

**Proposition 3.** Consider the bounds  $Y, Z(r) \in \mathbb{R}^6$  satisfying the component-wise inequalities (2.15). If  $\max_{j=1, \dots, 6} \{Z_j(r) + Y_j\} < r$ , then  $T : B_{\bar{a}}(r) \rightarrow B_{\bar{a}}(r)$  is a contraction. Moreover, there exists a unique  $\tilde{a} \in B_{\bar{a}}(r)$  such that  $F(\tilde{a}) = 0$ .

**Definition 1.** Given bounds  $Y$  and  $Z(r)$  satisfying (2.15), define  $p_1(r), \dots, p_6(r)$  by

$$p_j(r) \stackrel{\text{def}}{=} Z_j(r) - r + Y_j. \quad (2.16)$$

If for each  $j = 1, \dots, 6$ , the bound  $Z_j(r)$  is a polynomial in  $r$ , then  $p_j(r)$  is a polynomial in  $r$ . In this case, the polynomials  $p_1(r), \dots, p_6$  are called the *radii polynomials*.

The definition of the radii polynomials is based under the assumption that each component of the bound  $Z(r)$  can be obtained as a polynomial in  $r$ . We refer to Remark 1 in [1] for a justification of this assumption.

The next result, whose proof can be found in [1] provides an efficient mean of obtaining sets on which the Newton-like operator (2.14) is a contraction mapping.

**Proposition 4.** For a given exponential decay rate  $\nu \geq 1$ , construct the radii polynomials  $p_j = p_j(r)$  for  $j = 1, \dots, 6$  of Definition 1. Define

$$\mathcal{I} \stackrel{\text{def}}{=} \bigcap_{j=1}^6 \{r > 0 \mid p_j(r, \nu) < 0\}. \quad (2.17)$$

If  $\mathcal{I} \neq \emptyset$ , then  $\mathcal{I}$  is an open interval, and for any  $r \in \mathcal{I}$ , the ball  $B_{\tilde{x}}(r)$  contains a unique solution  $\tilde{x}$  such that  $F(\tilde{x}) = 0$ . Note that  $\tilde{x}$  is the same solution for all  $r \in \mathcal{I}$ .

We now derive the bounds  $Y_j$  and  $Z_j(r)$  for the definition of the radii polynomials which are defined in (2.15). Denote by  $\bar{a}$  the solution we found using Newton's method.

Recall that the bounds  $Y_j$  satisfy  $\|[T(\bar{a}) - \bar{a}]_j\|_\nu \leq Y_j$ , where  $T$  is our Newton-like operator. Recalling the action of each component of  $A$  given in (2.13), a direct computation yields the following computable bounds.

$$Y_1 \stackrel{\text{def}}{=} \sum_{k=0}^{m-1} \left| \sum_{i=1}^6 [A_{1, a_i}^{(m)} F_i^{(m)}(\bar{a})]_k \right| \nu^k \quad (2.18)$$

$$Y_2 \stackrel{\text{def}}{=} \sum_{k=0}^{m-1} \left| \sum_{i=1}^6 [A_{2, a_i}^{(m)} F_i^{(m)}(\bar{a})]_k \right| \nu^k + \sum_{k=m}^{4m-4} \frac{1}{k\omega} |[F_2(\bar{a})]_k| \quad (2.19)$$

$$Y_3 \stackrel{\text{def}}{=} \sum_{k=0}^{m-1} \left| \sum_{i=1}^6 [A_{3, a_i}^{(m)} F_i^{(m)}(\bar{a})]_k \right| \nu^k \quad (2.20)$$

$$Y_4 \stackrel{\text{def}}{=} \sum_{k=0}^{m-1} \left| \sum_{i=1}^6 [A_{4, a_i}^{(m)} F_i^{(m)}(\bar{a})]_k \right| \nu^k + \sum_{k=m}^{4m-4} \frac{1}{k\omega} |[F_4(\bar{a})]_k| \nu^k \quad (2.21)$$

$$Y_5 \stackrel{\text{def}}{=} \sum_{k=0}^{m-1} \left| \sum_{i=1}^6 [A_{5, a_i}^{(m)} F_i^{(m)}(\bar{a})]_k \right| \nu^k + \sum_{k=m}^{5m-5} \frac{1}{k\omega} |[F_5(\bar{a})]_k| \nu^k \quad (2.22)$$

$$Y_6 \stackrel{\text{def}}{=} \sum_{k=0}^{m-1} \left| \sum_{i=1}^6 [A_{6, a_i}^{(m)} F_i^{(m)}(\bar{a})]_k \right| \nu^k + \sum_{k=m}^{5m-5} \frac{1}{k\omega} |[F_6(\bar{a})]_k| \nu^k. \quad (2.23)$$

To compute the bounds  $Z_1(r), \dots, Z_6(r)$ , we have to bound each component of  $DF(\bar{a} + b)c$ , for  $b, c \in B(r)$ . We first note that:

$$DF(\bar{a} + b)c = (I - AA^\dagger)c - A(DF(\bar{a} + b) - A^\dagger)c$$

where  $A^\dagger$  is an approximation of  $DF(\bar{a})$ . Let  $B \stackrel{\text{def}}{=} I - AA^\dagger$ . This matrix has the form  $B = \{B_{j,a_i}\}_{i,j=1}^6$ . Note that given  $c \in X$ ,  $((Bc)_j)_k = 0$  for all  $k \geq m$ . By denoting  $b = \tilde{b}r$  and  $c = \tilde{c}r$  with  $\tilde{b}, \tilde{c} \in B_0(1)$ , we can deduce that for  $j = 1, \dots, 6$ , we have

$$\|(Bc)_j\|_\nu = \|(B\tilde{c})_j\|_\nu r \leq \left( \sum_{i=1}^6 \|B_{j,a_i}\|_{B(\ell_\nu^1, \ell_\nu^1)} \right) r = Z_j^{(0)} r \stackrel{\text{def}}{=} \left( \sum_{i=1}^6 K_{B,j,i} \right) r$$

where

$$K_{B,j,i} \stackrel{\text{def}}{=} \max_{0 \leq n \leq m-1} \frac{1}{\nu^n} \sum_{k=0}^{m-1} |(B_{j,a_i})_{k,n}| \nu^k.$$

Next, we need to bound  $\|[-A(DF(\bar{a} + b) - A^\dagger)c]_j\|_\nu$ , for  $j = 1, \dots, 6$ . For  $k \geq 1$ ,

$$\begin{aligned} [DF(\bar{a} + b)c]_1 &= k\omega(c_1)_k + (c_2)_k \\ [DF(\bar{a} + b)c]_2 &= k\omega(c_2)_k + 2(c_4)_k + (c_1)_k - (1 - \mu)[c_1(\bar{a}_5 + b_5)^3 + 3c_5(\bar{a}_1 + b_1)(\bar{a}_5 + b_5)^2]_k \\ &\quad - (\mu - \mu^2)[3c_5(\bar{a}_5 + b_5)^2]_k - \mu[c_1(\bar{a}_6 + b_6)^3 + 3c_6(\bar{a}_1 + b_1)(\bar{a}_6 + b_6)^2]_k \\ &\quad + (\mu - \mu^2)[3c_6(\bar{a}_6 + b_6)^2]_k \\ [DF(\bar{a} + b)c]_3 &= k\omega(c_3)_k + (c_4)_k \\ [DF(\bar{a} + b)c]_4 &= k\omega(c_4)_k + 2(c_2)_k - (c_3)_k + (1 - \mu)[c_3(\bar{a}_5 + b_5)^3 + 3c_5(\bar{a}_3 + b_3)(\bar{a}_5 + b_5)^2]_k \\ &\quad + \mu[c_3(\bar{a}_6 + b_6)^3 + 3c_6(\bar{a}_3 + b_3)(\bar{a}_6 + b_6)^2]_k \\ [DF(\bar{a} + b)c]_5 &= k\omega(c_5)_k + [c_1(\bar{a}_2 + b_2)(\bar{a}_5 + b_5)^3 + c_2(\bar{a}_1 + b_1)(\bar{a}_5 + b_5)^3 \\ &\quad + 3c_5(\bar{a}_1 + b_1)(\bar{a}_2 + b_2)(\bar{a}_5 + b_5)^2 + c_3(\bar{a}_4 + b_4)(\bar{a}_5 + b_5)^3 \\ &\quad + c_4(\bar{a}_3 + b_3)(\bar{a}_5 + b_5)^3 + 3c_5(\bar{a}_3 + b_3)(\bar{a}_4 + b_4)(\bar{a}_5 + b_5)^2]_k \\ &\quad + \mu[c_2(\bar{a}_5 + b_5)^3 + 3c_5(\bar{a}_2 + b_2)(\bar{a}_5 + b_5)^2]_k \\ [DF(\bar{a} + b)c]_6 &= k\omega(c_6)_k + [c_1(\bar{a}_2 + b_2)(\bar{a}_6 + b_6)^3 + c_2(\bar{a}_1 + b_1)(\bar{a}_6 + b_6)^3 \\ &\quad + 3c_6(\bar{a}_1 + b_1)(\bar{a}_2 + b_2)(\bar{a}_6 + b_6)^2 + c_3(\bar{a}_4 + b_4)(\bar{a}_6 + b_6)^3 \\ &\quad + c_4(\bar{a}_3 + b_3)(\bar{a}_6 + b_6)^3 + 3c_6(\bar{a}_3 + b_3)(\bar{a}_4 + b_4)(\bar{a}_6 + b_6)^2]_k \\ &\quad + (\mu - 1)[c_2(\bar{a}_6 + b_6)^3 + 3c_6(\bar{a}_2 + b_2)(\bar{a}_6 + b_6)^2]_k \end{aligned}$$

and

$$\begin{aligned} (A^\dagger c)_1 &= k\omega(c_1)_k + \{c_2\}_{k < m} \\ (A^\dagger c)_2 &= k\omega(c_2)_k + \{2(c_4) + (c_1) - (1 - \mu)(c_1\bar{a}_5^3) - 3(1 - \mu)(c_5\bar{a}_1\bar{a}_5^2) \\ &\quad - 3(\mu - \mu^2)(c_5\bar{a}_5^2) - \mu(c_1\bar{a}_6^3) - 3\mu(c_6\bar{a}_1\bar{a}_6^2) + 3(\mu - \mu^2)(c_6\bar{a}_6^2)\}_{k < m} \\ (A^\dagger c)_3 &= k\omega(c_3)_k + \{c_4\}_{k < m} \\ (A^\dagger c)_4 &= k\omega(c_4)_k + \{2(c_2) - (c_3) + (1 - \mu)(c_3\bar{a}_5^3) + 3(1 - \mu)(c_5\bar{a}_3\bar{a}_5^2) \\ &\quad + \mu(c_3\bar{a}_6^3) + 3\mu(c_6\bar{a}_3\bar{a}_6^2)\}_{k < m} \\ (A^\dagger c)_5 &= k\omega(c_5)_k + \{(c_1\bar{a}_2\bar{a}_5^3) + (c_2\bar{a}_1\bar{a}_5^3) + 3(c_5\bar{a}_1\bar{a}_2\bar{a}_5^2) + (c_3\bar{a}_4\bar{a}_5^3) + (c_4\bar{a}_3\bar{a}_5^3) \\ &\quad + 3(c_5\bar{a}_3\bar{a}_4\bar{a}_5^2) + \mu(c_2\bar{a}_5^2) + 3\mu(c_5\bar{a}_2\bar{a}_5^2)\}_{k < m} \\ (A^\dagger c)_6 &= k\omega(c_6)_k + \{(c_1\bar{a}_2\bar{a}_6^3) + (c_2\bar{a}_1\bar{a}_6^3) + 3(c_6\bar{a}_1\bar{a}_2\bar{a}_6^2) + (c_3\bar{a}_4\bar{a}_6^3) + (c_4\bar{a}_3\bar{a}_6^3) \\ &\quad + 3(c_6\bar{a}_3\bar{a}_4\bar{a}_6^2) + (\mu - 1)(c_2\bar{a}_6^2) + 3(\mu - 1)(c_6\bar{a}_2\bar{a}_6^2)\}_{k < m} \end{aligned}$$

Note moreover that for  $k = 0$ ,  $([DF(\bar{a} + b)c]_j - (A^\dagger c)_j)_0 = 0$  for  $j = 1, 3, 4$ . Also,

$$\begin{aligned}
([DF(\bar{a} + b)c]_5 - (A^\dagger c)_5)_0 &= \left[ \pm \left( 2 \sum_{k \geq m} (\tilde{c}_5)_k \right) \left( 2 \sum_{k=0}^{m-1} (\bar{a}_1)_k + \mu \right) \right. \\
&\quad \left. \pm \left( 2 \sum_{k \geq m} (\tilde{c}_1)_k \right) \left( 2 \sum_{k=0}^{m-1} (\bar{a}_1)_k \right) \right] r \\
&\quad + \left[ \pm \left( (\tilde{c}_5)_0 + 2 \sum_{k \geq 1} (\tilde{c}_5)_k \right) \left( (\tilde{b}_1)_0 + 2 \sum_{k \geq 1} (\tilde{b}_1)_k \right) \right. \\
&\quad \left. \pm \left( (\tilde{b}_5)_0 + 2 \sum_{k \geq 1} (\tilde{b}_5)_k \right) \left( (\tilde{c}_1)_0 + 2 \sum_{k \geq 1} (\tilde{c}_1)_k \right) \right] r^2.
\end{aligned}$$

Now, for  $a \in \ell_\nu^1$  such that  $\|a\|_\nu \leq 1$ , we have that

$$\left| a_0 + 2 \sum_{k \geq 1} a_k \right| \leq 2 \sum_{k \geq 0} |a_k| \leq 2 \sum_{k \geq 0} |a_k| \nu^k = 2 \|a\|_\nu \leq 2.$$

Hence,

$$|([DF(\bar{a} + b)c]_5 - (A^\dagger c)_5)_0| \leq \frac{2}{\nu^m} \left( \left| 2 \sum_{k=0}^{m-1} (\bar{a}_1)_k + \mu \right| + \left| 2 \sum_{k=0}^{m-1} (\bar{a}_1)_k \right| \right) r + 8r^2.$$

Similarly,

$$|([DF(\bar{a} + b)c]_6 - (A^\dagger c)_6)_0| \leq \frac{2}{\nu^m} \left( \left| 2 \sum_{k=0}^{m-1} (\bar{a}_1)_k + \mu - 1 \right| + \left| 2 \sum_{k=0}^{m-1} (\bar{a}_1)_k \right| \right) r + 8r^2.$$

Given an element  $a \in \ell_\nu^1$ , denote by  $a_F$  the finite-dimensional vector  $a_F = (a_0, a_1, \dots, a_{m-1})^T \in \mathbb{R}^m$ .

We now use the triangle inequality and Lemma 2 to bound  $\|[-A(DF(\bar{a} + b) - A^\dagger)c]_j\|_\nu$ . By substituting  $b$  and  $c$  with

$\tilde{b}r$  and  $\tilde{c}r$ , and grouping the corresponding powers of  $r$  together, we obtain that

$$\begin{aligned}
Z_j^{(1)} \stackrel{\text{def}}{=} & \frac{2}{\nu^m} \|(A_{j,a_5})_{:,0}\|_\nu \left( \left| 2 \sum_{k=0}^{m-1} (\bar{a}_1)_k + \mu \right| + \left| 2 \sum_{k=0}^{m-1} (\bar{a}_1)_k \right| \right) \\
& + \frac{2}{\nu^m} \|(A_{j,a_6})_{:,0}\|_\nu \left( \left| 2 \sum_{k=0}^{m-1} (\bar{a}_1)_k + \mu - 1 \right| + \left| 2 \sum_{k=0}^{m-1} (\bar{a}_1)_k \right| \right) \\
& + \frac{6}{m\omega} + |\mu - 1| \| |A_{j,a_2}| [|\bar{a}_5|^3 w]_F \|_\nu + 3|\mu - 1| \| |A_{j,a_2}| [|\bar{a}_1| |\bar{a}_5|^2 w]_F \|_\nu \\
& + 3|\mu^2 - \mu| \| |A_{j,a_2}| [|\bar{a}_5|^2 w]_F \|_\nu + \mu \| |A_{j,a_2}| [|\bar{a}_6|^3 w]_F \|_\nu + 3\mu \| |A_{j,a_2}| [|\bar{a}_1| |\bar{a}_6|^2 w]_F \|_\nu \\
& + 3|\mu^2 - \mu| \| |A_{j,a_2}| [|\bar{a}_6|^2 w]_F \|_\nu + |\mu - 1| \| |A_{j,a_4}| [|\bar{a}_5|^3 w]_F \|_\nu \\
& + 3|\mu - 1| \| |A_{j,a_4}| [|\bar{a}_3| |\bar{a}_5|^2 w]_F \|_\nu + \mu \| |A_{j,a_4}| [|\bar{a}_6|^3 w]_F \|_\nu + 3\mu \| |A_{j,a_4}| [|\bar{a}_3| |\bar{a}_6|^2 w]_F \|_\nu \\
& + \| |A_{j,a_5}| [|\bar{a}_1| |\bar{a}_5|^3 w]_F \|_\nu + \| |A_{j,a_5}| [|\bar{a}_2| |\bar{a}_5|^3 w]_F \|_\nu + \| |A_{j,a_5}| [|\bar{a}_3| |\bar{a}_5|^3 w]_F \|_\nu \\
& + \| |A_{j,a_5}| [|\bar{a}_4| |\bar{a}_5|^3 w]_F \|_\nu + 3 \| |A_{j,a_5}| [|\bar{a}_1| |\bar{a}_2| |\bar{a}_5|^2 w]_F \|_\nu \\
& + 3 \| |A_{j,a_5}| [|\bar{a}_3| |\bar{a}_4| |\bar{a}_5|^2 w]_F \|_\nu + \mu \| |A_{j,a_5}| [|\bar{a}_5|^3 w]_F \|_\nu + 3\mu \| |A_{j,a_5}| [|\bar{a}_2| |\bar{a}_5|^2 w]_F \|_\nu \\
& + \| |A_{j,a_6}| [|\bar{a}_1| |\bar{a}_6|^3 w]_F \|_\nu + \| |A_{j,a_6}| [|\bar{a}_2| |\bar{a}_6|^3 w]_F \|_\nu + \| |A_{j,a_6}| [|\bar{a}_3| |\bar{a}_6|^3 w]_F \|_\nu \\
& + \| |A_{j,a_6}| [|\bar{a}_4| |\bar{a}_6|^3 w]_F \|_\nu + 3 \| |A_{j,a_6}| [|\bar{a}_1| |\bar{a}_2| |\bar{a}_6|^2 w]_F \|_\nu \\
& + 3 \| |A_{j,a_6}| [|\bar{a}_3| |\bar{a}_4| |\bar{a}_6|^2 w]_F \|_\nu + |\mu - 1| \| |A_{j,a_6}| [|\bar{a}_6|^3 w]_F \|_\nu \\
& + 3|\mu - 1| \| |A_{j,a_6}| [|\bar{a}_2| |\bar{a}_6|^2 w]_F \|_\nu,
\end{aligned} \tag{2.24}$$

where  $(A_{j,a_i})_{:,0} \in \ell_\nu^1$  is the first *column* of the operator for  $i = 5, 6$ , and where  $w \stackrel{\text{def}}{=} (0, 0, \dots, 0, \frac{1}{\nu^m}, \frac{1}{\nu^{m+1}}, \frac{1}{\nu^{m+2}}, \dots)$ .

$$\begin{aligned}
Z_j^{(2)} \stackrel{\text{def}}{=} & 8 \left( \| (A_{j,a_5})_{:,0} \|_\nu + \| (A_{j,a_6})_{:,0} \|_\nu \right) \\
& + 4 \| |A_{j,a_2}| [|\mu - 1| (24 \|\bar{a}_5\|_\nu^2 + 24 \|\bar{a}_1\|_\nu \|\bar{a}_5\|_\nu) + 6|\mu^2 - \mu| \|\bar{a}_5\|_\nu \\
& + 24\mu (\|\bar{a}_6\|_\nu^2 + \|\bar{a}_1\|_\nu \|\bar{a}_6\|_\nu) + 6|\mu^2 - \mu| \|\bar{a}_6\|_\nu ] \\
& + 4 \| |A_{j,a_4}| [|\mu - 1| (24 \|\bar{a}_5\|_\nu^2 + 24 \|\bar{a}_3\|_\nu \|\bar{a}_5\|_\nu) + 24\mu (\|\bar{a}_6\|_\nu^2 + \|\bar{a}_3\|_\nu \|\bar{a}_6\|_\nu) ] \\
& + 4 \| |A_{j,a_5}| [64 \|\bar{a}_5\|_\nu^3 + 24 \|\bar{a}_5\|_\nu^2 (4 \|\bar{a}_1\|_\nu + 4 \|\bar{a}_2\|_\nu + 4 \|\bar{a}_3\|_\nu + 4 \|\bar{a}_4\|_\nu + \mu) \\
& + 24 \|\bar{a}_5\|_\nu (\mu \|\bar{a}_2\|_\nu + 4 \|\bar{a}_1\|_\nu \|\bar{a}_2\|_\nu + 4 \|\bar{a}_3\|_\nu \|\bar{a}_4\|_\nu) ] \\
& + 4 \| |A_{j,a_6}| [64 \|\bar{a}_6\|_\nu^3 + 24 \|\bar{a}_6\|_\nu^2 (4 \|\bar{a}_1\|_\nu + 4 \|\bar{a}_2\|_\nu + 4 \|\bar{a}_3\|_\nu + 4 \|\bar{a}_4\|_\nu + |\mu - 1|) \\
& + 24 \|\bar{a}_6\|_\nu (|\mu - 1| \|\bar{a}_2\|_\nu + 4 \|\bar{a}_1\|_\nu \|\bar{a}_2\|_\nu + 4 \|\bar{a}_3\|_\nu \|\bar{a}_4\|_\nu) ],
\end{aligned} \tag{2.25}$$

$$\begin{aligned}
Z_j^{(3)} \stackrel{\text{def}}{=} & 16 \| |A_{j,a_2}| [9|\mu - 1| \|\bar{a}_5\|_\nu + 9\mu \|\bar{a}_6\|_\nu + 3|\mu - 1| \|\bar{a}_1\|_\nu + 3\mu \|\bar{a}_1\|_\nu + 3|\mu^2 - \mu| ] \\
& + 16 \| |A_{j,a_4}| [9|\mu - 1| \|\bar{a}_5\|_\nu + 9\mu \|\bar{a}_6\|_\nu + 3\mu \|\bar{a}_3\|_\nu ] \\
& + 16 \| |A_{j,a_5}| [72 \|\bar{a}_5\|_\nu^2 + 9 \|\bar{a}_5\|_\nu (4 \|\bar{a}_1\|_\nu + 4 \|\bar{a}_2\|_\nu + 4 \|\bar{a}_3\|_\nu + 4 \|\bar{a}_4\|_\nu + \mu) \\
& + 3\mu \|\bar{a}_2\|_\nu + 12 \|\bar{a}_1\|_\nu \|\bar{a}_2\|_\nu + 12 \|\bar{a}_3\|_\nu \|\bar{a}_4\|_\nu ] \\
& + 16 \| |A_{j,a_6}| [72 \|\bar{a}_6\|_\nu^2 + 9 \|\bar{a}_6\|_\nu (4 \|\bar{a}_1\|_\nu + 4 \|\bar{a}_2\|_\nu + 4 \|\bar{a}_3\|_\nu + 4 \|\bar{a}_4\|_\nu + |\mu - 1|) \\
& + 3|\mu - 1| \|\bar{a}_2\|_\nu + 12 \|\bar{a}_1\|_\nu \|\bar{a}_2\|_\nu + 12 \|\bar{a}_3\|_\nu \|\bar{a}_4\|_\nu ],
\end{aligned} \tag{2.26}$$

$$\begin{aligned}
Z_j^{(4)} \stackrel{\text{def}}{=} & 64 |8\mu - 1| \| |A_{j,a_2}| \| + 64 |8\mu - 1| \| |A_{j,a_4}| \| \\
& + 64 \| |A_{j,a_5}| [24 \|\bar{a}_5\|_\nu + 4 \|\bar{a}_1\|_\nu + 4 \|\bar{a}_2\|_\nu + 4 \|\bar{a}_3\|_\nu + 4 \|\bar{a}_4\|_\nu + 4\mu] \\
& + 64 \| |A_{j,a_6}| [24 \|\bar{a}_6\|_\nu + 4 \|\bar{a}_1\|_\nu + 4 \|\bar{a}_2\|_\nu + 4 \|\bar{a}_3\|_\nu + 4 \|\bar{a}_4\|_\nu + 4|\mu - 1|],
\end{aligned} \tag{2.27}$$

$$Z_j^{(5)} \stackrel{\text{def}}{=} 2560(\|A_{j,a_5}\| + \|A_{j,a_6}\|). \quad (2.28)$$

Combining (2.18), (2.19), (2.20), (2.21), (2.22), (2.23), (2.24), (2.25), (2.26), (2.27) and (2.28), we define, for each  $j = 1, \dots, 6$ , the quintic radii polynomial  $p_j(r)$  by

$$p_j(r) \stackrel{\text{def}}{=} Z_j^{(5)} r^5 + Z_j^{(4)} r^4 + Z_j^{(3)} r^3 + Z_j^{(2)} r^2 + (Z_j^{(1)} - 1) r + Y_j. \quad (2.29)$$

## 2.6 Results

In this section, we present some application of the radii polynomial approach. Using a computer program in MATLAB together with the interval arithmetic toolbox INTLAB, we compute the radii polynomials  $p_1(r), \dots, p_6(r)$  given by (2.29), and we apply Proposition 4 to prove existence of periodic solutions of the planar circular restricted 3-body problem (2.1). We proved the existence of periodic orbits in the case where the two large bodies have the same mass, that is the mass ratio is  $\mu = \frac{1}{2}$ . These orbits are shown in Figure 5. Moreover, we proved the existence of periodic orbits in the earth-moon system, that is with the mass ratio  $\mu = 0.0123$ . These orbits are shown in Figure 6.

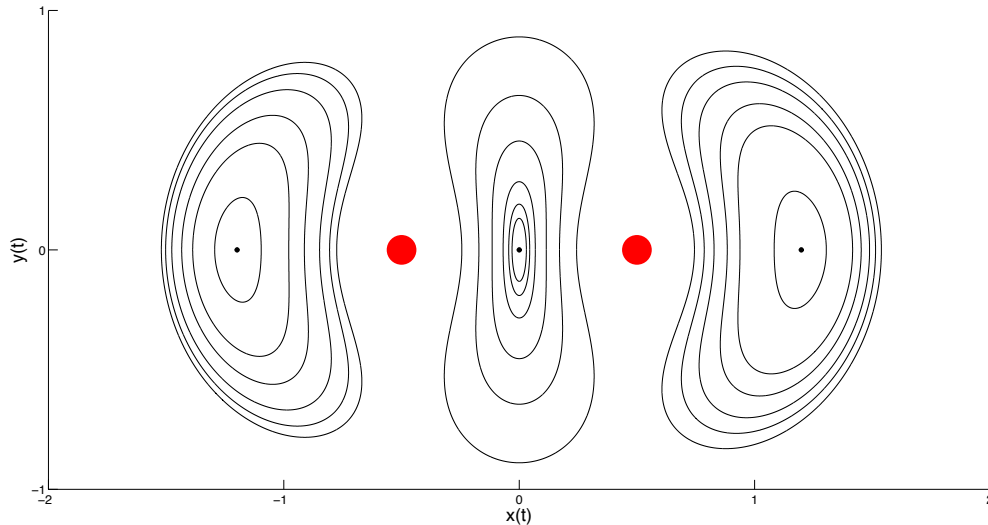


Figure 5: In this figure, we show the picture of several rigorously computed periodic orbits for the planar circular restricted 3-body problem (2.1). The mass ratio between the bodies is  $\mu = 0.5$  which corresponds to two bodies with equal mass. The largest periodic orbit of the left family has frequency  $\omega \approx 1.276$ , and is proven with 149 Fourier coefficients,  $\nu = 1.01$  and  $r = 2.9 \times 10^{-10}$ . The largest periodic orbit of the center family has frequency  $\omega \approx 1.283$ , and is proven with 157 Fourier coefficients,  $\nu = 1.015$  and  $r = 4.5 \times 10^{-9}$ . The largest periodic orbit of the right family has frequency  $\omega \approx 1.286$ , and is proven with 122 Fourier coefficients,  $\nu = 1.01$  and  $r = 2.5 \times 10^{-9}$ .

## References

- [1] Allan Hungria, Jean-Philippe Lessard, and Jason D. Mireles-James. Rigorous numerics for analytic solutions of differential equations: the radii polynomial approach. To appear in *Math. Comp.*, 2015.
- [2] Gianni Arioli. Periodic orbits, symbolic dynamics and topological entropy for the restricted 3-body problem. *Comm. Math. Phys.*, 231(1):1–24, 2002.

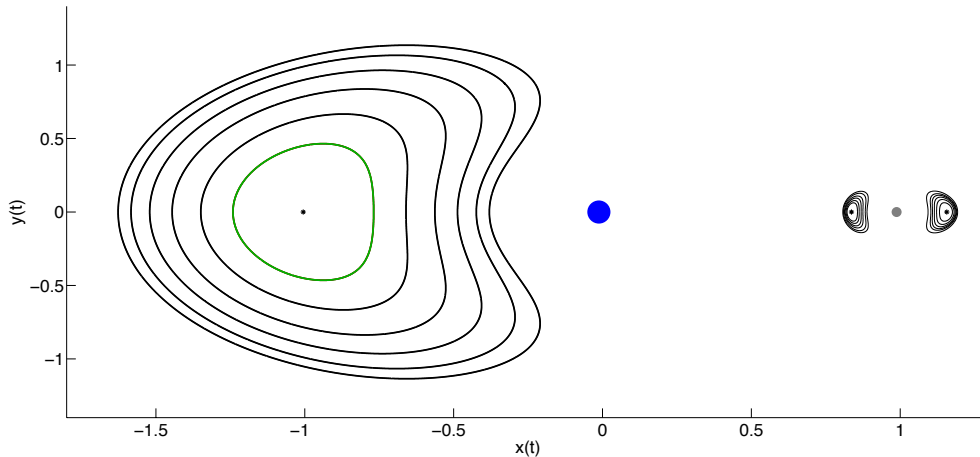


Figure 6: In this figure, we show the picture of several rigorously computed periodic orbits for the planar circular restricted 3-body problem (2.1). The mass ratio between the bodies is  $\mu = 0.0123$  which corresponds to the earth-moon mass ratio. (The sizes of the dots indicating the earth and the moon are not shown to scale). The largest periodic orbit of the left family has frequency  $\omega \approx 1.0079$ , and is proven with 130 Fourier coefficients,  $\nu = 1.012$  and  $r = 6.1 \times 10^{-9}$ . The largest periodic orbit of the center family has frequency  $\omega \approx 2.0614$ , and is proven with 61 Fourier coefficients,  $\nu = 1.02$  and  $r = 1.75 \times 10^{-9}$ . The largest periodic orbit of the right family has frequency  $\omega \approx 1.7906$ , and is proven with 58 Fourier coefficients,  $\nu = 1.013$  and  $r = 3.52 \times 10^{-10}$ .

- [3] Gianni Arioli. Branches of periodic orbits for the planar restricted 3-body problem. *Discrete Contin. Dyn. Syst.*, 11(4):745–755, 2004.
- [4] Daniel Wilczak and Piotr Zgliczynski. Heteroclinic connections between periodic orbits in planar restricted circular three-body problem—a computer assisted proof. *Comm. Math. Phys.*, 234(1):37–75, 2003.
- [5] Daniel Wilczak and Piotr Zgliczyński. Heteroclinic connections between periodic orbits in planar restricted circular three body problem. II. *Comm. Math. Phys.*, 259(3):561–576, 2005.
- [6] Maciej J. Capiński. Computer assisted existence proofs of Lyapunov orbits at  $L_2$  and transversal intersections of invariant manifolds in the Jupiter-Sun PCR3BP. *SIAM J. Appl. Dyn. Syst.*, 11(4):1723–1753, 2012.
- [7] Jean-Philippe Lessard and Christian Reinhardt. Rigorous Numerics for Nonlinear Differential Equations Using Chebyshev Series. *SIAM J. Numer. Anal.*, 52(1):1–22, 2014.
- [8] Jan Bouwe van den Berg and Jean-Philippe Lessard. Chaotic braided solutions via rigorous numerics: chaos in the Swift-Hohenberg equation. *SIAM J. Appl. Dyn. Syst.*, 7(3):988–1031, 2008.
- [9] Sarah Day, Jean-Philippe Lessard, and Konstantin Mischaikow. Validated continuation for equilibria of PDEs. *SIAM J. Numer. Anal.*, 45(4):1398–1424 (electronic), 2007.
- [10] Marcio Gameiro and Jean-Philippe Lessard. Rigorous computation of smooth branches of equilibria for the three dimensional Cahn-Hilliard equation. *Numer. Math.*, 117(4):753–778, 2011.
- [11] Marcio Gameiro and Jean-Philippe Lessard. Analytic estimates and rigorous continuation for equilibria of higher-dimensional PDEs. *J. Differential Equations*, 249(9):2237–2268, 2010.

- [12] Jan Bouwe van den Berg, Chris M. Groothedde, and J. F. Williams. Rigorous computation of a radially symmetric localised solution in a Ginzburg-Landau problem. *SIAM J. Appl. Dyn. Syst.*, 14(1): 423–447, 2015.
- [13] Marcio Gameiro and Jean-Philippe Lessard. Efficient Rigorous Numerics for Higher-Dimensional PDEs via One-Dimensional Estimates. *SIAM J. Numer. Anal.*, 51(4):2063–2087, 2013.
- [14] Lorenzo D’Ambrosio, Jean-Philippe Lessard, and Alessandro Pugliese. Blow-up profile for solutions of a fourth order nonlinear equation. To appear in *Nonlinear Anal.*, 2015.
- [15] Marcio Gameiro, Jean-Philippe Lessard, and Yann Ricaud. Rigorous numerics for piecewise-smooth systems: a functional analytic approach based on Chebyshev series. Submitted., 2015.
- [16] Rafael de la Llave, Jordi-Lluís Figueras, Marcio Gameiro, and Jean-Philippe Lessard. Theoretical results on the numerical computation and a-posteriori verification of invariant objects of evolution equations. *In preparation.*, 2015.
- [17] Roberto Castelli and Jean-Philippe Lessard. Rigorous Numerics in Floquet Theory: Computing Stable and Unstable Bundles of Periodic Orbits. *SIAM J. Appl. Dyn. Syst.*, 12(1):204–245, 2013.
- [18] Gábor Kiss and Jean-Philippe Lessard. Computational fixed-point theory for differential delay equations with multiple time lags. *J. Differential Equations*, 252(4):3093–3115, 2012.
- [19] Jean-Philippe Lessard. Recent advances about the uniqueness of the slowly oscillating periodic solutions of Wright’s equation. *J. Differential Equations*, 248(5):992–1016, 2010.
- [20] J. B. Van den Berg, J. D. Mireles James, and Christian Reinhardt. A parameterized newton-kantorovich method for rigorously computing (un)stable manifolds: non-resonant and resonant spectra. (*In preparation*), 2015.
- [21] Anaïs Correc and Jean-Philippe Lessard. Coexistence of nontrivial solutions of the one-dimensional Ginzburg-Landau equation: a computer-assisted proof. *European J. Appl. Math.*, 26(1):33–60, February 2015.
- [22] Roberto Castelli and Holger Teismann. Rigorous numerics for NLS: bound states, spectra, and controllability. Preprint, 2013.
- [23] Roberto Castelli and Jean-Philippe Lessard. A method to rigorously enclose eigenpairs of complex interval matrices. In *Applications of mathematics 2013*, pages 21–31. Acad. Sci. Czech Repub. Inst. Math., Prague, 2013.
- [24] Jean-Philippe Lessard, Jason D. Mireles James, and Christian Reinhardt. Computer assisted proof of transverse saddle-to-saddle connecting orbits for first order vector fields. *J. Dynam. Differential Equations*, 26(2):267–313, 2014.
- [25] Jan Bouwe van den Berg, Jason D. Mireles-James, Jean-Philippe Lessard, and Konstantin Mischaikow. Rigorous numerics for symmetric connecting orbits: even homoclinics of the Gray-Scott equation. *SIAM J. Math. Anal.*, 43(4):1557–1594, 2011.
- [26] Jan Bouwe van den Berg, Andréa Deschênes, Jean-Philippe Lessard, and Jason D. Mireles James. Stationary coexistence of hexagons and rolls via rigorous computations. To appear in *SIAM J. Appl. Dyn. Syst.*, 2015.
- [27] Marcio Gameiro, Jean-Philippe Lessard, and Alessandro Pugliese. Computation of smooth manifolds of solutions of PDEs via rigorous multi-parameter continuation. To appear in *Found. Comput. Math.*, 2015.
- [28] Jan Bouwe van den Berg, Jean-Philippe Lessard, and Konstantin Mischaikow. Global smooth solution curves using rigorous branch following. *Math. Comp.*, 79(271):1565–1584, 2010.
- [29] Maxime Breden, Jean-Philippe Lessard, and Matthieu Vanicat. Global Bifurcation Diagrams of Steady States of Systems of PDEs via Rigorous Numerics: a 3-Component Reaction-Diffusion System. *Acta Appl. Math.*, 128:113–152, 2013.

- [30] Donald E. Knuth. *The art of computer programming. Vol. 2.* Addison-Wesley Publishing Co., Reading, Mass., second edition, 1981. Seminumerical algorithms, Addison-Wesley Series in Computer Science and Information Processing.
- [31] Martin Bückner, George Corliss, Paul Hovland, Uwe Naumann, and Boyana Norris, editors. *Automatic differentiation: applications, theory, and implementations*, volume 50 of *Lecture Notes in Computational Science and Engineering*. Springer-Verlag, Berlin, 2006. Papers from the 4th International Conference on Automatic Differentiation held in Chicago, IL, July 20–24, 2004.
- [32] Àngel Jorba and Maorong Zou. A software package for the numerical integration of ODEs by means of high-order Taylor methods. *Experiment. Math.*, 14(1):99–117, 2005.
- [33] A. Haro. Automatic differentiation methods in computational dynamical systems: Invariant manifolds and normal forms of vector fields at fixed points. *Manuscript*.
- [34] Warwick Tucker. *Validated numerics*. Princeton University Press, Princeton, NJ, 2011. A short introduction to rigorous computations.
- [35] Martin Berz and Kyoko Makino. Verified integration of ODEs and flows using differential algebraic methods on high-order Taylor models. *Reliab. Comput.*, 4(4):361–369, 1998.
- [36] Kyoko Makino and Martin Berz. Taylor models and other validated functional inclusion methods. *Int. J. Pure Appl. Math.*, 4(4):379–456, 2003.
- [37] A. Wittig, M. Berz, J. Grote, K. Makino, and S. Newhouse. Rigorous and accurate enclosure of invariant manifolds on surfaces. *Regul. Chaotic Dyn.*, 15(2-3):107–126, 2010.
- [38] Piotr Zgliczynski.  $C^1$  Lohner algorithm. *Found. Comput. Math.*, 2(4):429–465, 2002.
- [39] Piotr Zgliczyński. Rigorous numerics for dissipative partial differential equations. II. Periodic orbit for the Kuramoto-Sivashinsky PDE—a computer-assisted proof. *Found. Comput. Math.*, 4(2):157–185, 2004.
- [40] S.M. Rump. INTLAB - INTerval LABoratory. In Tibor Csendes, editor, *Developments in Reliable Computing*, pages 77–104. Kluwer Academic Publishers, Dordrecht, 1999. <http://www.ti3.tu-harburg.de/rump/>.
- [41] R. de la Llave and D. Rana. Accurate strategies for K.A.M. bounds and their implementation. In *Computer aided proofs in analysis (Cincinnati, OH, 1989)*, volume 28 of *IMA Vol. Math. Appl.*, pages 127–146. Springer, New York, 1991.
- [42] Kenneth R. Meyer and Dieter S. Schmidt, editors. *Computer aided proofs in analysis*, volume 28 of *The IMA Volumes in Mathematics and its Applications*. Springer-Verlag, New York, 1991.
- [43] Hans Koch, Alain Schenkel, and Peter Wittwer. Computer-assisted proofs in analysis and programming in logic: a case study. *SIAM Rev.*, 38(4):565–604, 1996.
- [44] Gianni Arioli and Hans Koch. Integration of dissipative partial differential equations: a case study. *SIAM J. Appl. Dyn. Syst.*, 9(3):1119–1133, 2010.
- [45] Kenneth R. Meyer, Glen R. Hall, and Dan Offin. *Introduction to Hamiltonian dynamical systems and the N-body problem*, volume 90 of *Applied Mathematical Sciences*. Springer, New York, second edition, 2009.
- [46] Antonio Fasano and Stefano Marmi. *Analytical mechanics*. Oxford Graduate Texts. Oxford University Press, Oxford, 2013. An introduction, Translated from the 2002 Italian original by Beatrice Pelloni, Paperback edition of the 2006 English translation [2010 reprint, MR2849188].
- [47] J.-P. Lessard, J.D. Mireles James and J. Ransford, MATLAB codes available at <http://archimede.mat.ulaval.ca/jplessard/AD/>